ELSEVIER

Chemical Engineering Journal 67 (1997) 27–36

Chemical Engineering Journal

Extension of the Wong-Sandler mixing rule to the three-parameter Patel-Teja equation of state: Application up to the near-critical region

T. Yang, G.-J. Chen, W. Yan, T.-M. Guo *

High Pressure Fluid Phase Behavior and Property Research Laboratory, University of Petroleum, P.O. Box 902, Beijing 100083, People's Republic of China

Received 1 August 1996; accepted 19 December 1996

Abstract

The Wong-Sandler mixing rule was extended to the Patel-Teja three-parameter cubic equation of state by introducing suitable corresponding parameters. The new model, PT–WS model, has been extensively tested on various classes of binary/ternary mixtures, special attention was paid to the effects on the representation of mixture phase behavior in the near-critical region. The test results indicate that the new model is capable of improving both the vapor–liquid equilibrium and volumetric properties significantly, especially for highly asymmetric systems. The proposed method of implementing the Wong-Sandler mixing rule can be applied to other multi-parameter cubic equations of state.

Keywords: Equation of state; Mixing rule; Phase behavior; Near-critical region

1. Introduction

Since Huron and Vidal [1] introduced the excess free energy model into cubic equation of state (EOS), the development of a local composition type mixing rule for complex systems became a hot research area, and a number of review articles are available [2–4]. Among the existing mixing rules, the density-independent Wong-Sandler (WS) mixing rule [5,6] received particular attention. The chief advantage of the WS mixing rule is its capability of extending the available g^E-model parameter values determined from low pressure vapor–liquid equilibrium (VLE) data to high pressure systems. In addition, at the low pressure limit, the classic quadratic mixing rule for the second virial coefficient can be recovered. However, the reported applications of the WS mixing rule were limited to two-parameter cubic equations of state.

For improving the description of the fluid phase behavior in the near-critical region, Chou and Prausnitz [7], Mathias et al. [8] and Chu et al. [9] introduced various correction functions into the cubic EOS. Although those functions work well for pure components, the extension to mixtures is often unsatisfactory.

The major objective of this work is to apply the WS mixing rule to the three-parameter cubic EOS proposed by Patel and Teja [10], and study the capability of improving the representation of VLE and volumetric properties of various classes of mixtures, emphasis is placed on the performance in the near-critical region and the effects on highly asymmetric systems.

2. Derivation of Wong-Sandler type mixing rules for the Patel-Teja EOS parameters

The Patel-Teja equation of state (PT EOS) is in the following form

$$P=\frac{RT}{v-b}-\frac{a(T)}{v(v+b)+c(v-b)} \tag{1}$$

The following relationship between the second virial coefficient (B) and the parameters a and b in the van der Waals (vdW) type EOS can be derived

$$B=b-\frac{a}{RT} \tag{2}$$

For mixtures

$$B_m=b_m-\frac{a_m}{RT} \tag{3}$$

* Corresponding author. Tel.: +86 10 62320066extn.2828; fax: +86 10 62311421; e-mail: guotm@upcl.ihep.ac.cn

1385-8947/97/$17.00
PII S1385-8947(97)00012-0

Table 1
The parameter ξ in various two-parameter cubic EOS

Equation of state	ξ
vdW (1873)	1
PR (1976)	$\frac{1}{2\sqrt{2}} \ln \frac{2+\sqrt{2}}{2-\sqrt{2}}$
SRK (1972)	ln 2

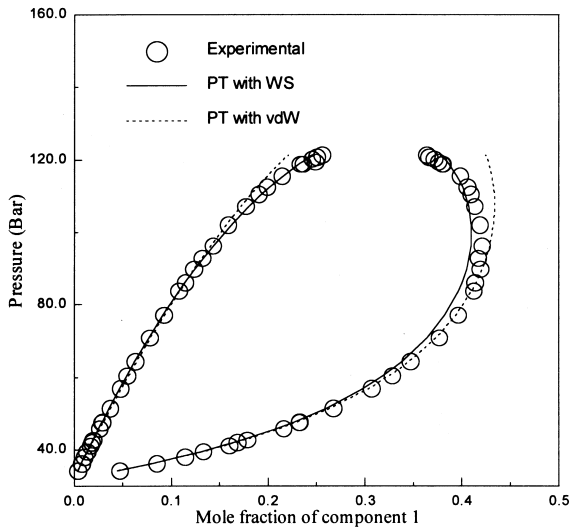

Fig. 1. Coexisting vapor–liquid phase compositions under various pressures ($N_2(1)$–$CO_2(2)$ binary system, $T=270$ K).

Based on statistical mechanics, the following quadratic mixing rule was derived for the second virial coefficient

$$B_m = \sum_i \sum_j x_i x_j B_{ij} \tag{4}$$

where the cross coefficient B_{ij} is evaluated by

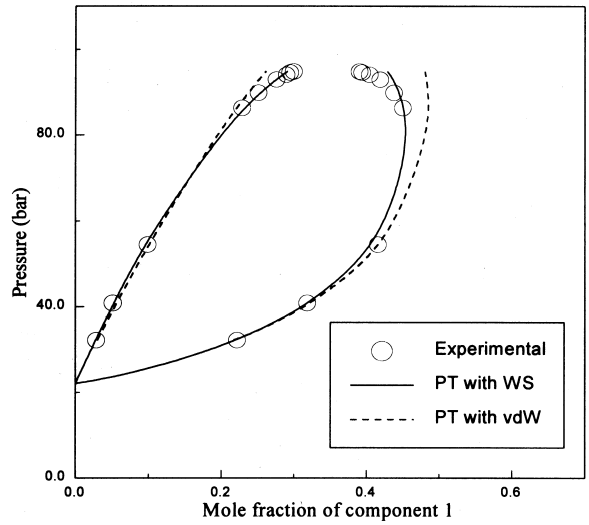

Fig. 2. Coexisting vapor–liquid phase compositions under various pressures ($N_2(1)$–$C_2H_6(2)$ binary system, $T=270$ K).

$$B_{ij} = \frac{B_i + B_j}{2}(1 - k_{ij}) \tag{5}$$

the correction term $(1-k_{ij})$ was introduced by Wong and Sandler [5,6]. Equating Eqs. (3) and (4) yields

$$b_m - \frac{a_m}{RT} = \sum_i \sum_j x_i x_j B_{ij} \tag{6}$$

Define d and e as follows

$$d = \frac{-(b+c) + \sqrt{b^2 + 6bc + c^2}}{2} \tag{7}$$

$$e = \frac{-(b+c) - \sqrt{b^2 + 6bc + c^2}}{2} \tag{8}$$

then the PT EOS can be expressed in the following form

Table 2
Correlation of the vapor–liquid equilibria for non-polar binary systems — PT–WS model

System	N_p	Temperature range (K)	Pressure range (bar)	τ_{12}	τ_{21}	k_{ij}	*ADD-P* (%)	Δy	Data [a] source
N_2–CO_2	41	270–293	34–121	0.0501	1.1683	0.258	0.75	0.0081	[1]
CO_2–C_3H_8	22	277–344	7–65	0.1804	0.6590	0.394	1.37	0.0059	[2]
CH_4–nC_4H_{10}	34	327–344	7–128	1.7458	−0.8886	0.508	1.58	0.0075	[3]
CO_2–nC_4H_{10}	22	283–377	9–82	1.4871	0.0961	0.413	2.53	0.0137	[1], [4]
CH_4–CO_2	10	270	32–83	1.6300	0.1517	0.111	0.48	0.0112	[5]
nC_4H_{10}–$nC_{10}H_{22}$	6	344	0–8	1.9672	−0.9361	0.264	0.67	0.0047	[6]
CO_2–$nC_{10}H_{22}$	21	344	64–128	3.9293	−0.6751	0.719	0.31	0.0032	[7]
CO_2–$cycC_6H_{12}$	8	366	18–128	3.0891	−0.5677	0.488	3.18	0.0128	[8]
N_2–nC_4H_{10}	10	410	35–69	4.5585	0.4387	0.700	0.23	0.0158	[1]
N_2–CH_4	7	170	23–30	−1.7642	1.5631	0.711	0.57	0.0059	[9]
CO_2–$cycC_6H_{12}$	10	410	17–145	3.4883	−0.8081	0.486	2.16	0.0130	[8]
N_2–nC_4H_{10}	12	310	11–285	0.9501	0.2958	0.594	3.29	0.0274	[1]
nC_4H_{10}–nC_8H_{18}	14	339–400	9–20	2.7205	−0.9612	0.060	1.17	–	[10]
CO_2–C_2H_6	14	269	22–36	0.9274	0.0655	0.276	0.16	–	[11]
N_2–C_2H_6	10	270	22–95	−0.1404	1.0702	0.473	0.73	0.0085	[12]
CH_4–nC_8H_{18}	5	348	30–71	−0.3786	0.6307	0.744	0.10	0.0029	[13]

[a] See Appendix C.

$$P=\frac{RT}{v-b}-\frac{a}{d-e}\left(\frac{1}{v-d}-\frac{1}{v-e}\right) \quad (9)$$

From basic thermodynamic relationships and Eq. (9), the residual Helmholtz free energy function can be derived

$$A^{R}=\left(-\int_{V=\infty}^{V}P\mathrm{d}v\right)-\left(-\int_{V=\infty}^{V=RT/P}\frac{RT}{v}\mathrm{d}v\right)$$
$$=-RT\ln\left[\frac{P(v-b)}{RT}\right]-\frac{a}{d-e}\ln\frac{v-e}{v-d} \quad (10)$$

Under infinite pressure, Eq. (10) is reduced to the following form

$$A^{R}_{\infty}=-\frac{a}{d-e}\ln\frac{b-e}{b-d} \quad (11)$$

For mixture

$$A^{R}_{\infty m}=-\frac{a_m}{d_m-e_m}\ln\frac{b_m-e_m}{b_m-d_m} \quad (12)$$

For going further in the derivation, the following corresponding parameters ψ_i and ξ_i were introduced for pure component i

$$\psi_i=\frac{c_i}{b_i} \quad (13)$$

$$\xi_i=\frac{1}{\sqrt{1+6\psi_i+\psi_i^2}}\ln\frac{3+\psi_i+\sqrt{1+6\psi_i+\psi_i^2}}{3+\psi_i-\sqrt{1+6\psi_i+\psi_i^2}} \quad (14)$$

for mixtures, the simple linear combining rule was chosen for the corresponding parameter ψ_m

$$\psi_m=\sum_i x_i\psi_i \quad (15)$$

and thus

$$c_m=\psi_m b_m \quad (16)$$

$$\xi_m=\frac{1}{\sqrt{1+6\psi_m+\psi_m^2}}\ln\frac{3+\psi_m+\sqrt{1+6\psi_m+\psi_m^2}}{3+\psi_m-\sqrt{1+6\psi_m+\psi_m^2}} \quad (17)$$

Based on the definition of excess Helmholtz free energy (A^{E}) and by substituting the above mentioned defining equa-

Table 3
Correlation of the vapor–liquid equilibria for nonpolar–polar binary systems — PT–WS model

System	N_p	Temperature range (K)	Pressure range (bar)	τ_{12}	τ_{21}	k_{ij}	*ADD-P* (%)	Δy	Data [a] source
C_2H_6–CH_3OH	5	298	10–41	−0.1582	1.9059	0.347	1.09	0.0007	[14]
CO_2–H_2O	12	543	200–1200	0.3467	2.4059	0.417	0.97	0.0232	[15]
C_3H_8–C_2H_5OH	22	400–425	7–59	2.5937	−0.4612	−0.018	1.73	0.0264	[16]
iC_4H_{10}–CH_3OH	23	323–423	1–46	5.6890	2.4756	−0.166	2.35	0.0543	[17]
CO_2–CH_3OH	17	298–313	6–81	0.7185	0.0479	0.380	3.60	0.0015	[18]
N_2–CH_3OH	10	250–273	24–179	−0.2614	3.1757	−0.449	1.95	0.0224	[19]
C_3H_8–CH_3OH[b]	21	313–343	4–25	−0.4399	2.0861	0.567	3.77	0.0199	[20]
nC_5H_{12}–C_3H_6O[c]	9	238	0.01–0.04	2.0369	2.0295	0.152	1.33	0.0087	[21]
CH_3OH–cC_6H_{12}	9	298	0.13–0.29	2.1630	2.6328	0.369	4.63	0.0375	[22]

[a] See Appendix C.
[b] $\alpha=0.47$.
[c] τ_{12} and τ_{21} values were taken from DECHEMA data series, α's were set equal to 0.4683 and 0.4231, respectively.

Table 4
Correlation/prediction of the vapor–liquid equilibria for polar–polar binary systems — PT–WS model

System	N_p	Temperature range (K)	Pressure range (bar)	k_{ij}	*ADD-P* (%)	Δy	Data [a] source
CH_3OH–H_2O	13	298	0.04–0.16	0.089	1.98	0.0076	[23]
CH_3OH–H_2O [b]	10	373	1.0–3.4	–	1.15	0.0166	[23]
CH_3OH–H_2O [b]	16	523	17–83	–	2.93	0.0114	[23]
C_3H_6O–H_2O	22	373	1.1–3.7	0.255	1.89	0.0067	[23]
C_3H_6O–H_2O [b]	15	523	40–68	–	4.70	0.0217	[23]
C_3H_6O–CH_3OH	14	298	0.17–0.31	0.077	0.78	0.0081	[23]
C_3H_6O–CH_3OH [b]	14	373	3.5–4.0	–	7.23	0.0168	[23]
C_3H_6O–CH_3OH [b]	10	473	3.5–4.0	–	6.51	0.0411	[23]
C_2H_5OH–H_2O	5	348	0.59–0.89	0.276	1.35	0.0115	[24]
C_3H_6O–$CHCl_3$	11	308	0.33–0.87	−0.080	0.87	0.0050	[25]
NH_3–H_2O [c]	28	526	47–210	−0.156	1.75	0.0353	[26]

[a] See Appendix C.
[b] Prediction based on τ_{12} and τ_{21} values regressed from low-pressure VLE data (DECHEMA data series).
[c] $\tau_{12}=-1.0506$, $\tau_{21}=0.7322$, $\alpha=0.3$.

Table 5
Correlation of the vapor–liquid equilibria for binary systems containing hydrogen sulfide — PT–WS model

System	N_p	Temperature range (K)	Pressure range (bar)	τ_{12}	τ_{21}	k_{ij}	*ADD-P* (%)	Δy	Data [a] source
N_2–H_2S	18	321–344	41–190	0.3246	2.2604	0.428	0.69	0.0320	[27]
H_2S–nC_7H_{16}	21	352–394	11–84	0.7777	0.4520	0.575	0.76	0.0044	[28]
H_2S–nC_5H_{12}	31	377–444	14–90	0.1878	0.5617	0.471	2.06	0.0346	[29]
H_2S–$nC_{10}H_{22}$	16	410–444	14–124	2.9553	−0.9199	0.672	1.23	0.0020	[30]
H_2S–iC_4H_{10}	17	310–344	7–51	2.9190	−0.0756	0.112	1.04	0.0242	[31]
CO_2–H_2S	12	266–280	14–34	0.8174	0.8522	0.023	0.80	0.0136	[32]
CH_4–H_2S	6	270	31–57	−1.9357	5.4687	1.042	1.23	0.0904	[33]

[a] See Appendix C.

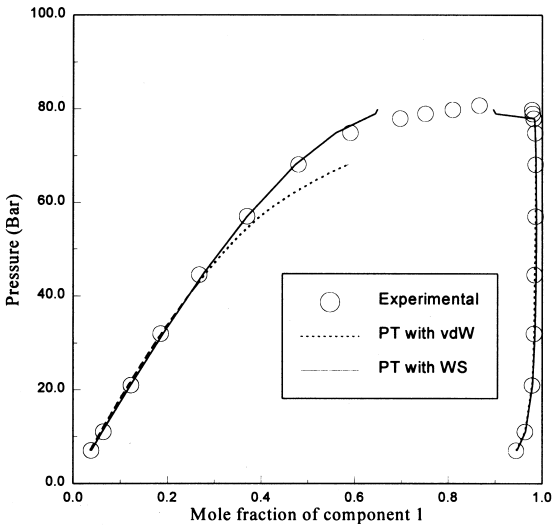

Fig. 3. Coexisting vapor–liquid phase compositions under various pressures (CO_2(1)–CH_3OH(2) binary system, T = 313 K).

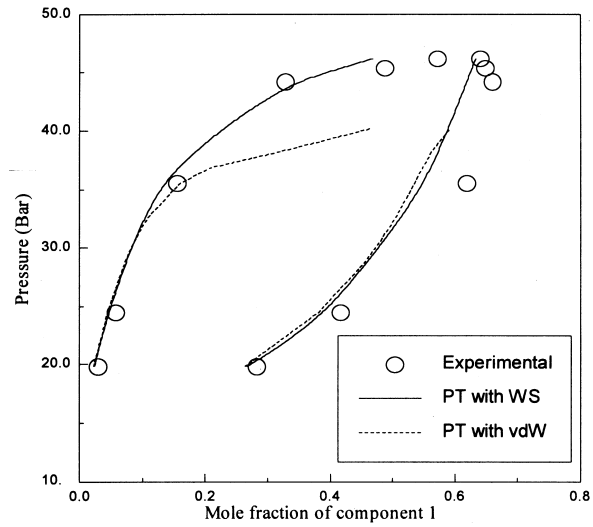

Fig. 4. Coexisting vapor–liquid phase compositions under various pressures (iC_4H_{10}(1)–CH_3OH(2) binary system, T = 423 K).

tions into Eqs. (11) and (12), the expression for A^E_∞ was as follows

$$A^E_\infty = -\xi_m \frac{a_m}{b_m} + \sum_i x_i \xi_i \frac{a_i}{b_i} \tag{18}$$

Equating Eqs. (6) and (18), the following Wong-Sandler type mixing rules for parameters a_m and b_m in the PT EOS can be derived

$$b_m = \frac{\sum_i \sum_j x_i x_j \left(b - \frac{a}{RT}\right)_{ij}}{1 + \frac{1}{\xi_m RT}\left(A^E_\infty - \sum_i x_i \xi_i \frac{a_i}{b_i}\right)} \tag{19}$$

$$a_m = \frac{b_m}{\xi_m}\left(-A^E_\infty + \sum_i x_i \xi_i \frac{a_i}{b_i}\right) \tag{20}$$

Eqs. (5), (19) and (20), together with the defining equations for corresponding parameters, Eqs. (13)–(17), constitute a complete set of the new mixing rules for the PT EOS. Existing g^E/A^E models can be applied to represent the A^E_∞ function in the mixing rules. In this work, the NRTL model proposed by Renon et al. [11] was chosen. When the NRTL

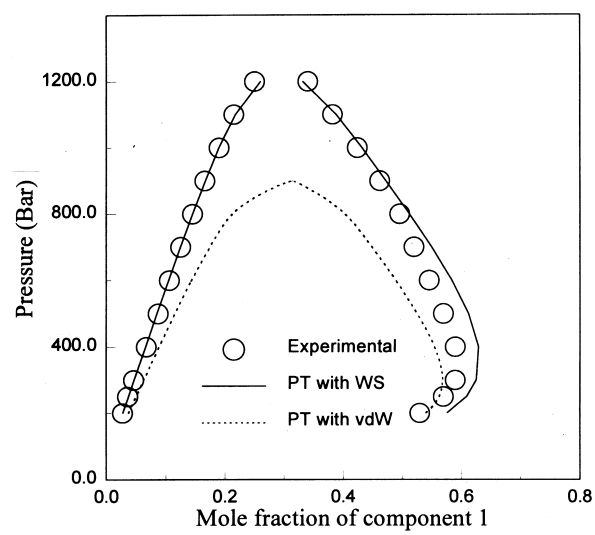

Fig. 5. Coexisting vapor–liquid phase compositions under various pressures (CO_2(1)–H_2O(2) binary system, T = 543 K).

parameters (τ_{12}, τ_{21} and α) determined at low pressure conditions were taken directly from the literature (e.g. the DECHEMA data series), the binary interaction coefficient k_{ij} in Eq. (5) was adjusted to match the experimental VLE data.

Table 6
Prediction results on the vapor–liquid equilibria of ternary systems — PT–WS model

System	N_p	Temperature range (K)	Pressure range (bar)	*AAD-P* (%)	Δy	Data [a] source
N_2–CO_2–C_2H_6	40	270	84–96	3.11	0.0161	[12]
N_2–CO_2–nC_4H_{10}	18	310	137–275	2.42	0.0276	[1]
N_2–CO_2–nC_4H_{10}	5	410	62	1.81	0.0103	[1]
N_2–CH_4–CO_2	36	270	85–110	2.34	0.0037	[34]
CO_2–nC_4H_{10}–$nC_{10}H_{22}$	11	344	100–115	1.52	0.0115	[35]
CH_4–nC_4H_{10}–nC_8H_{18}	5	353	50–160	4.54	0.0122	[36]
CH_4–CO_2–H_2S	3	270	41–64	12.86	0.0268	[33]
CH_4O–C_3H_6O–H_2O	15	523	47–82	5.46	0.0298	[23]
CO_2–C_3H_8–CH_4O	24	313	5–32	8.01	0.0320	[20]

[a] See Appendix C.

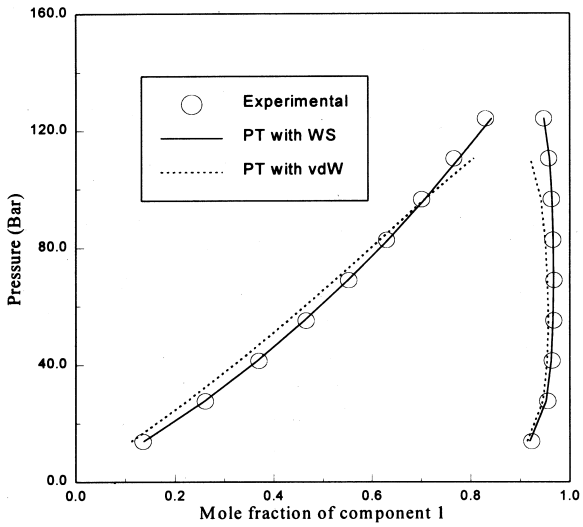

Fig. 6. Coexisting vapor–liquid phase compositions under various pressures ($H_2S(1)$–$nC_{10}H_{22}(2)$ binary system, $T = 444$ K).

The derivation of the expression for the fugacity coefficient (φ_i) corresponding to the PT–WS model is given in Appendix B.

The proposed method of developing Wong–Sandler type mixing rules for the PT EOS can be applied to other multiparameter as well as two-parameter cubic equations of state, the expressions of the corresponding parameter ξ for the vdW, PR and SRK equations of state are given in Table 1.

3. Applications

The performance of the proposed PT–WS model has been tested on the vapor–liquid equilibrium and volumetric data of various classes of mixtures covering wide ranges of pressure and temperature. Special attention was given to the phase behavior in the near-critical region and the effects on highly asymmetric systems. The optimal values for NRTL parameters τ_{12} and τ_{21}, if not available in the literature, were determined simultaneously with the binary interaction coefficient k_{ij} from binary VLE data. The modified Levenberg–Marquadt nonlinear least squares regression method was applied in the data reduction, the objective function (F) used was

$$F = \sum_{j=1}^{N_p} \left[\frac{(P_{exp} - P_{cal})}{P_{exp}} \right]_j^2 \quad (21)$$

The third parameter α in the NRTL model was set equal to 0.3, if not otherwise specified. The deviations, *AAD-P* (%) and Δy in the subsequent tables are defined as follows

$$AAD - P(\%) = \frac{1}{N_{p_{j=1}}} \sum^{N_p} \left| \frac{P_{cal} - P_{exp}}{P_{exp}} \right|_j \times 100 \quad (22)$$

$$\Delta y = \frac{1}{N_{p_{j=1}}} \sum^{N_p} |y_{cal} - y_{exp}|_j \quad (23)$$

Table 7
Prediction results on the coexisting vapor–liquid phase densities — PT–WS model

System	N_p	Temperature range (K)	Pressure range (bar)	*AAD* (%) of vapor phase density	*AAD* (%) of liquid phase density	Data [a] source
CH_4–nC_4H_{10}	18	327	7–128	2.98	1.87	[3]
N_2–nC_4H_{10}	11	311	11–285	1.93	5.31	[1]
H_2S–nC_5H_{12}	12	377	14–90	7.34	5.26	[29]
H_2S–$nC_{10}H_{22}$	9	444	14–110	2.03	5.13	[30]
CO_2–nC_4H_{10}–$nC_{10}H_{22}$	15	344	100–115	3.10	5.47	[35]
N_2–CO_2–nC_4H_{10}	32	311	107–275	3.66	2.79	[1]

[a] See Appendix C.

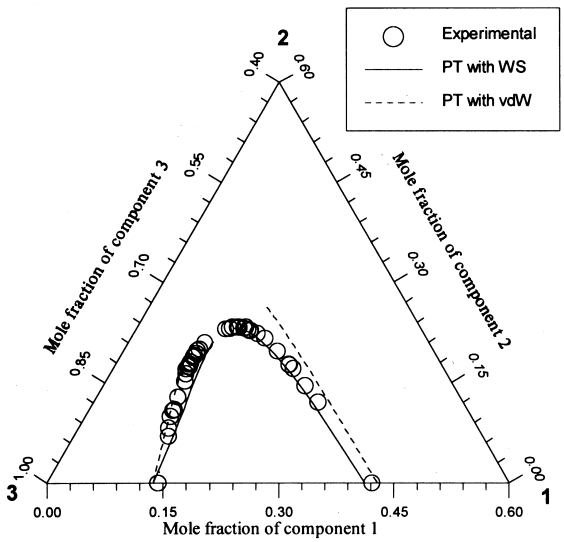

Fig. 7. Coexisting vapor–liquid phase compositions ($N_2(1)$–$CH_4(2)$–$CO_2(3)$ ternary system, $T=270$ K, $P=95$ bar).

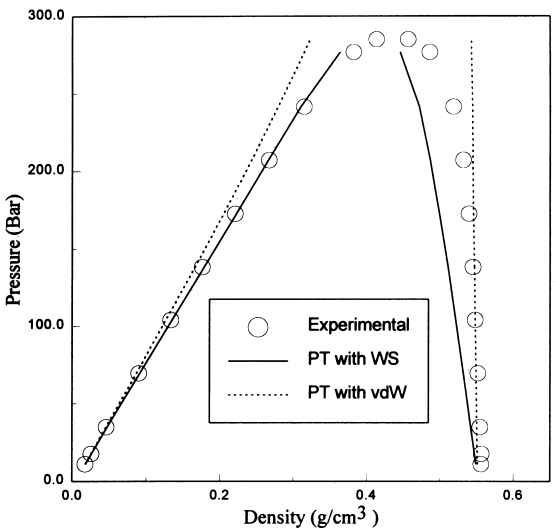

Fig. 8. Coexisting vapor–liquid phase densities (N_2–nC_4H_{10} binary system, $T=311$ K).

3.1. Non-polar binary systems

The correlation results on the VLE data of 16 non-polar binary systems are listed in Table 2. Typical comparisons with the performance of PT–vdW model (PT EOS coupled with van der Waals one fluid mixing rule) are presented in Figs. 1 and 2. The improvement achieved by the PT–WS model in the near-critical region is quite impressive.

3.2. Binary systems containing polar component(s)

The correlation/prediction results on the VLE data of 9 nonpolar–polar and 11 polar–polar binary systems are listed in Tables 3 and 4, respectively. The prediction results indicate the excellent extrapolating ability of the PT–WS model. Typical comparisons with the PT–vdW model are depicted in

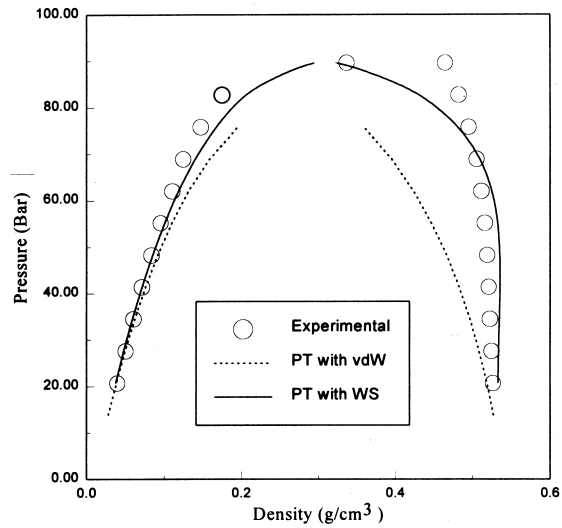

Fig. 9. Coexisting vapor–liquid phase densities (H_2S–nC_5H_{12} binary system, $T=377$ K).

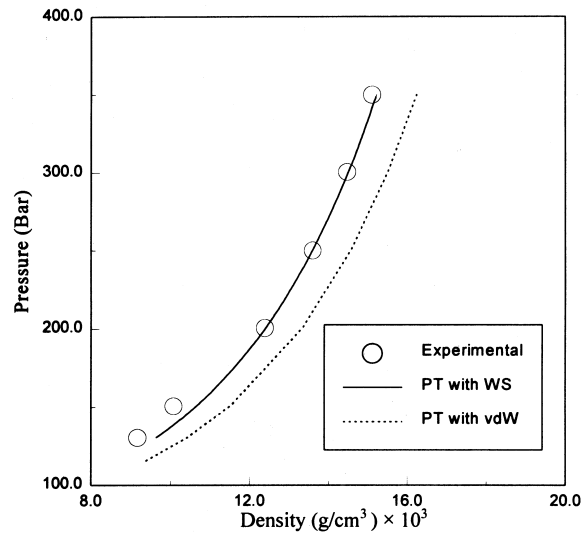

Fig. 10. Density of fluid in the compressed fluid region (CH_4–CO_2–nC_4H_{10} ternary system, $T=301$ K).

Figs. 3–5, the PT–WS model again shows superiority in the near-critical region.

3.3. Binary systems containing hydrogen sulfide

The correlation results on the VLE data of 7 binary systems containing hydrogen sulfide are listed in Table 5. Typical comparisons with the PT–vdW model are given in Fig. 6, significant improvement in the near-critical region is again observed.

3.4. Prediction on the VLE of ternary systems

Table 6 lists the VLE prediction results for 9 ternary systems based on the parameter values determined from related binary systems. Due to the excellent extrapolating capability of Wong–Sandler mixing rule, the predictions of the PT–WS

Table 8
Prediction results on the compressed fluid density for the CH_4–CO_2–nC_4H_{10} ternary system — PT–WS model

Temperature (K)	Pressure (bar)	Density cald. (mol/cm^3) $\times 10^3$	
		Exp. data [a]	PT–WS
294.55	351.6	15.586	15.687
	301.6	14.986	14.996
	251.2	14.195	14.131
	201.4	13.143	13.006
	151.4	11.411	11.354
	131.4	10.278	10.402
	ADD(%)		0.65
300.55	350.0	15.301	15.223
	300.6	14.633	14.509
	250.2	13.799	13.600
	200.5	12.656	12.412
	150.6	10.724	10.656
	130.5	9.531	9.638
	ADD(%)		1.99
308.45	349.0	14.828	14.639
	299.1	14.164	13.879
	249.1	13.241	12.924
	199.4	11.957	11.661
	149.4	9.846	9.788
	129.4	8.592	8.724
	115.4	7.530	7.812
	ADD(%)		2.00

[a] Pan et al. [12].

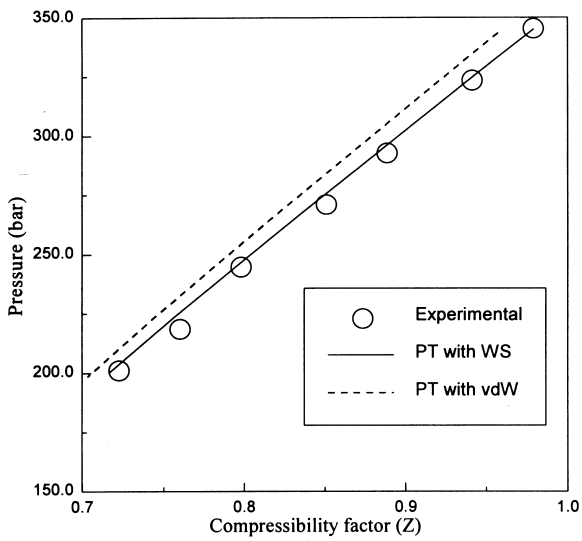

Fig. 11. Compressibility factor of fluid in the compressed fluid region (CH_4–nC_4H_{10}–nC_8H_{18} ternary system, $T = 343$ K).

model are not sensitive to the temperature/pressure range of the experimental data used in binary parameters regression.

For the selected ternary systems in Table 6, the PT–WS model gives satisfactory representation of VLE data up to the near-critical region. Typical comparison with the PT–vdW model is presented in Fig. 7, the converging approach of the coexisting vapor–liquid composition is well described by the PT–WS model.

Table 9
Prediction results on the compressibility factor of compressed fluid for the CH_4–nC_4H_{10}–nC_8H_{18} ternary system — PT–WS model

Temperature (K)	Pressure (bar)	Compressibility factor (Z)	
		Exp. data [a]	PT–WS
323.1	350.6	1.022	0.975
	329.1	0.977	0.932
	301.3	0.918	0.877
	272.6	0.859	0.819
	249.9	0.812	0.773
	224.9	0.762	0.724
	203.0	0.720	0.680
	ADD(%)	–	2.73
342.6	343.4	0.977	0.971
	324.5	0.941	0.936
	296.6	0.889	0.884
	273.3	0.846	0.841
	247.1	0.799	0.794
	221.9	0.757	0.749
	198.5	0.722	0.708
	ADD(%)	–	0.83
362.2	341.4	1.004	0.982
	316.3	0.959	0.939
	291.2	0.917	0.896
	269.9	0.877	0.860
	241.4	0.837	0.814
	217.2	0.802	0.776
	192.3	0.772	0.740
	182.6	0.769	0.727
	ADD(%)		3.01

[a] Yang [13].

3.5. Prediction on the density of equilibrium phases

For the binary and ternary systems tested in Table 7, the PT–WS model gives good predictions for the coexisting phase densities, especially for the highly asymmetric systems. Typical comparisons with the PT–vdW model are shown in Figs. 8 and 9, the improvement of liquid phase density prediction by the PT–WS model in the near-critical region is very impressive.

3.6. Prediction on the compressed fluid density/compressibility factor for ternary systems

The prediction results on the compressed fluid density/compressibility factor for two ternary mixtures at various temperatures and pressures are listed in Tables 8 and 9, respectively. The improvements over the PT–vdW model are illustrated in Figs. 10 and 11.

4. Conclusions

The procedure of developing the Wong–Sandler type mixing rule for the three-parameter Patel–Teja equation of state

has been established, and can be extended to other multi-parameter as well as two-parameter cubic equations of state.

The extensive test results on the VLE and volumetric calculations for binary and ternary systems indicate that the proposed PT–WS model is capable of describing both the VLE and the volumetric properties satisfactorily for various classes of mixtures. As compared with the PT–vdW model, the improvements achieved in the near-critical region and for the highly asymmetric systems are particularly impressive.

Acknowledgements

The financial support received from the National Science Foundation of China and the China National Petroleum and Natural Gas Corporation is gratefully acknowledged.

Appendix A. Nomenclature

a	PT EOS parameter
A	Helmholtz free energy
b	PT EOS parameter
B	second virial coefficient
c	PT EOS parameter
d	defined by Eq. (7)
D	defined by Eq. (B-3)
e	defined by Eq. (8)
F	objective function
k_{ij}	binary interaction coefficient
n	mole number
N_p	number of data points
P	pressure
Q	defined by Eq. (B-2)
R	gas constant
T	temperature
V	molar volume
x	mole fraction
y	mole fraction in vapor phase
Z	compressibility factor

Greek letters

α	parameter in the NRTL g^E model
ψ	parameter defined by Eq. (13)
γ	activity coefficient
φ	fugacity coefficient
ξ	parameter defined by Eq. (14)
τ_{ij}	interaction parameter in NRTL model

Subscripts

c	critical property
cal	calculated value
exp	experimental value
i	molecular species
j	molecular species
ij	interaction between molecules i and j
m	mixture
r	reduced property
T	total
∞	at infinite pressure

Superscripts

E	excess property
R	residual property

Appendix B. The derivation of the expression for component fugacity coefficient (φ_i) corresponding to the PT–WS model

The derivation of the expression for component fugacity coefficient (φ_i) corresponding to the PT–WS model is briefly described below:

$$RT\ln\varphi_i = RT\ln\frac{V}{V-b_m} + RT\left[\frac{\partial(n_T b_m)}{\partial n_i}\right]\frac{1}{V-b_m} + \left[\frac{\frac{1}{n}\left[\frac{\partial(n_T^2 a)}{\partial n_i}\right]}{d_m-e_m} - \frac{a_m\left[\frac{\partial(n_T d_m)}{\partial n_i} - \frac{\partial(n_T e_m)}{\partial n_i}\right]}{((d_m-e_m))^2}\right]\ln\frac{V-d_m}{V-e_m}$$

$$-\frac{a_m\left[\frac{\partial(n_T d_m)}{\partial n_i}\right]}{(v-d_m)(d_m-e_m)} + \frac{a_m\left[\frac{\partial(n_T e_m)}{\partial n_i}\right]}{(v-e_m)(d_m-e_m)} - RT\ln Z \qquad \text{(B-1)}$$

with Q and D defined as:

$$Q = \sum_i\sum_j x_i x_j\left(b - \frac{a}{RT}\right)_{ij} \qquad \text{(B-2)}$$

$$D = \frac{1}{\xi_m RT}\left(\sum_i x_i\xi_i\frac{a_i}{b_i} - A_\infty^E\right) \qquad \text{(B-3)}$$

The partial derivatives in Eq. (B-1) are evaluated as follows

$$\frac{\partial(n_T b_m)}{\partial n_i}=\frac{1}{1-D}\left(\frac{1}{n_T}\frac{\partial(n_T^2 Q)}{\partial n_i}\right)-\frac{Q}{(1-D)^2}\left(1-\frac{\partial(n_T D)}{\partial n_i}\right) \tag{B-4}$$

$$\frac{1}{n_T}\left(\frac{\partial(n_T^2 a_m)}{\partial n_i}\right)=RT\left(D\frac{\partial(n_T b_m)}{\partial n_i}+b_m\frac{\partial(n_T D)}{\partial n_i}\right) \tag{B-5}$$

$$\frac{1}{n_T}\left(\frac{\partial(n_T^2 Q)}{\partial n_i}\right)=2\sum_j x_j\left(b-\frac{a}{RT}\right)_{ij} \tag{B-6}$$

$$\frac{\partial(n_T D)}{\partial n_i}=\frac{\xi_i\dfrac{a_i}{b_i}-RT\ln\gamma_{\infty i}}{\xi_m RT}-\frac{n_T RT\left(\sum_i x_i\xi_i\dfrac{a_i}{b_i}\right)\left(\dfrac{\partial\xi_m}{\partial n_i}\right)}{(\xi_m RT)^2} \tag{B-7}$$

$$n_T\left(\frac{\partial\xi_m}{\partial n_i}\right)=-\frac{3\dfrac{c_i}{b_i}-3\psi_m+\dfrac{c_i}{b_i}\psi_m-\psi_m^2}{\sqrt{(1+6\psi_m+\psi_m^2)^3}}\ln\frac{3+\psi_m+\sqrt{1+6\psi_m+\psi_m^2}}{3+\psi_m-\sqrt{1+6\psi_m+\psi_m^2}}+\frac{1}{\sqrt{1+6\psi_m+\psi_m^2}} \tag{B-8}$$

$$\times\left[\frac{(\psi_i-\psi_m)+\dfrac{3\dfrac{c_i}{b_i}-3\psi_m+\dfrac{c_i}{b_i}\psi_m-\psi_m^2}{\sqrt{1+6\psi_m+\psi_m^2}}}{3+\psi_m+\sqrt{1+6\psi_m+\psi_m^2}}-\frac{(\psi_i-\psi_m)-\dfrac{3\dfrac{c_i}{b_i}-3\psi_m+\dfrac{c_i}{b_i}\psi_m-\psi_m^2}{\sqrt{1+6\psi_m+\psi_m^2}}}{3+\psi_m-\sqrt{1+6\psi_m+\psi_m^2}}\right] \tag{B-8}$$

$$\frac{\partial(n_T c_m)}{\partial n_i}=\frac{\partial(n_T b_m)}{\partial n_i}\sum_i x_i\frac{c_i}{b_i}+b_m\frac{c_i}{b_i}-b_m\sum_i x_i\frac{c_i}{b_i} \tag{B-9}$$

$$\frac{\partial(n_T d_m)}{\partial n_i}=\frac{1}{2}\left[-\left(\frac{\partial(n_T b_m)}{\partial n_i}+\frac{\partial(n_T c_m)}{\partial n_i}\right)+\frac{b_m\dfrac{\partial(n_T b_m)}{\partial n_i}+3b_m\dfrac{\partial(n_T c_m)}{\partial n_i}+3c_m\dfrac{\partial(n_T b_m)}{\partial n_i}+c_m\dfrac{\partial(n_T c_m)}{\partial n_i}}{\sqrt{b_m^2+6b_m c_m+c_m^2}}\right] \tag{B-10}$$

$$\frac{\partial(n_T e_m)}{\partial n_i}=\frac{1}{2}\left[-\left(\frac{\partial(n_T b_m)}{\partial n_i}+\frac{\partial(n_T c_m)}{\partial n_i}\right)-\frac{b_m\dfrac{\partial(n_T b_m)}{\partial n_i}+3b_m\dfrac{\partial(n_T c_m)}{\partial n_i}+3c_m\dfrac{\partial(n_T b_m)}{\partial n_i}+c_m\dfrac{\partial(n_T c_m)}{\partial n_i}}{\sqrt{b_m^2+6b_m c_m+c_m^2}}\right] \tag{B-11}$$

Appendix C. Data sources

C.1. Table C-1. Experimental data sources

[1] Shibata, S.K. and Sandler, S.I., *J. Chem. Eng. Data* 34 (1989) 291.
[2] Reamer, H.H. et al., *Ind. Eng. Chem.* 42 (1950) 534.
[3] Sage, B.H. and Lacey, W.N., *API research project* 37 (1950).
[4] Davalos, J. et al., *J. Chem. Eng. Data* 21 (1976) 81.
[5] Brown, T.S. et al., *Fluid Phase Equilibria* 53 (1989) 7.
[6] Reamer, H.H. et al., *J. Chem. Eng. Data* 9 (1964) 24.
[7] Nagarajan, N. and Robinson, R.L. Jr., *J. Chem. Eng. Data* 30 (1986) 168.
[8] Shibata, S.K. and Sandler, S.I., *J. Chem. Eng. Data* 34 (1989) 419.
[9] Kidnay, A.F. et al., *Cryogenics* 15 (1975) 531–540.
[10] Kay, W.B. et al., *J. Chem. Eng. Data* 19 (1974) 275–280.
[11] Gugnoni, R.J. et al., *AIChE J.* 20 (1974) 357–362.
[12] Brown, T.S. et al., *Fluid Phase Equilibria* 51 (1989) 299–313.
[13] Kohn, J.P. et al., *J. Chem. Eng. Data* 9 (1964) 5.
[14] Ohgaki, K. et al., *J. Chem. Eng. Data* 21 (1976) 55.
[15] Takenouchi, S. and Kennedy, G.C., *Am. J. Sci.* 262 (1964) 1055.
[16] Gomez-Nieto, M. and Thodos, G., *AIChE J.* 24 (1978) 672–678.
[17] Leu, A.-D. and Robinson, D.B., *J. Chem. Eng. Data* 37 (1990) 10–13.
[18] Ohgaki, K. et al., *J. Chem. Eng. Data* 21 (1976) 53.

[19] Weber, W. et al., *Fluid Phase Equilibria* 18 (1984) 253–278.
[20] Galivel-Solastiouk, F. et al., *Fluid Phase Equilibria* 28 (1986) 73–85.
[21] Raal, W., Schaefer, K., *Z. Elektrochem.* 63 (1959) 1019.
[22] Kurtyniva, L.M. et al., *Khim. Thermodin. Rastvorov* 2 (1968) 43.
[23] Griswold, J. et al., *J. Chem. Eng. Prog. Symp. Ser.* 48 (1952) 18–34.
[24] Nikokaya, A.V., *Zh. Fiz. Khim* 20 (1946) 421.
[25] Kuoryavtseva, L.S. and Susarev, M.P., *Zh. Prikl. Khim.* 36 (1963) 1231.
[26] Rizvi, S.S.H. et al., *J. Chem. Eng. Data* 32 (1987) 183–191.
[27] Besserer, G.J. and Robinson, D.B., *J. Chem. Eng. Data* 20 (1975) 157.
[28] Ng, H.-J. et al., *J. Chem. Eng. Data* 25 (1980) 51.
[29] Reamer, H.H. et al., *Ind. Eng. Chem.* 45 (1953) 1805.
[30] Reamer, H.H. et al., *Ind. Eng. Chem.* 45 (1953) 1810.
[31] Robinson, D.B. et al., *Nat. Gas Proc. Ass. Res. Rep. Rp.* 7 (1972).
[32] Sobocinski, D.P. et al., *AIChE J.* 5 (1959) 545.
[33] Morris, J.S. et al., *Fluid Phase Equilibria* 66 (1991) 291.
[34] Somait, F.A. and Kidnay, A.J., *J. Chem. Eng. Data* 23 (1978) 301–305.
[35] Nigarajan, N. et al., *J. Chem. Eng. Data* 35 (1990) 228–231.
[36] Yang, T. et al., submitted to *Chem. Eng. Sci.* (1996).

References

[1] M.J. Huron, J. Vidal, Fluid Phase Equilibria 3 (1979) 255–271.
[2] K. Knudsen, E.H. Stenby, A. Fredenslund, Fluid Phase Equilibria 82 (1992) 361–368.
[3] R.A. Heidmann, Proceedings of the Seventh International Conference on Fluid Properties and Phase Equilibria for Chemical Process Design, 1995, Snowmass, Colorado, USA, pp. 295–300.
[4] H.-Q. Pan, T.-M. Guo, Chem. Eng. J. 61 (1996) 213–225.
[5] D.S.H. Wong, S.I. Sandler, AIChE J. 38 (1992) 671–680.
[6] D.S.H. Wong, H. Orbey, S.I. Sandler, Ind. Eng. Chem. Res. 31 (1992) 2033–2039.
[7] G.F. Chou, J.M. Prausnitz, AIChE J. 35 (1989) 1487–1496.
[8] P.M. Mathias, T. Naheri, E.M. Oh, Fluid Phase Equilibria 47 (1989) 77–87.
[9] J.-Z. Chu, Y.-X. Zuo, T.-M. Guo, Fluid Phase Equilibria 77 (1992) 181–216.
[10] N.C. Patel, A.S. Teja, Chem. Eng. Sci. 37 (1982) 463–473.
[11] H. Renon, J.M. Prausnitz, AIChE J. (1965) 135–144.
[12] H.-Q. Pan, T. Yang, T.-M. Guo, Fluid Phase Equilibria 105 (1995) 259–271.
[13] T. Yang, Ph.D. Thesis, University of Petroleum, Beijing, 1996.